Asociación Argentina
de Mecánica Computacional

Mecánica Computacional Vol XXX, págs. 2275-2288 (artículo completo)
Oscar Möller, Javier W. Signorelli, Mario A. Storti (Eds.)
Rosario, Argentina, 1-4 Noviembre 2011

GENERATION OF TURBULENT INLET VELOCITY CONDITIONS FOR LARGE EDDY SIMULATIONS

Hugo G. Castro[a,b], Rodrigo R. Paz[a] and Victorio E. Sonzogni[a]

[a]*Centro Internacional de Métodos Computacionales en Ingeniería (CIMEC), INTEC-CONICET-UNL, Güemes 3450, (S300GLN), Santa Fe, Argentina. http://www.cimec.org.ar*

[b]*Grupo de Investigacin en Mecnica de Fluidos, Universidad Tecnológica Nacional, Facultad Regional Resistencia. Chaco, Argentina. hugoguillermo_castro@yahoo.com.ar*

Keywords: Turbulence Synthesis, Inlet Boundary Conditions, Navier-Stokes Equations, LES method.

Abstract. We present a methodology for the generation of synthesized turbulence at inflow boundaries when simulating fluid flow problems using the Large Eddy Simulation (LES) method. A key point of the proposed technique is that the statistical properties of turbulence are properly represented, keeping even the anisotropy characteristics that the turbulent flow may possess. The computational cost is comparable to the other approaches in which this method is based.

The strategy of imposing conditions on the inlet velocity field through turbulence synthesis was implemented in the parallel multiphysics code called PETSc-FEM (http://www.cimec.org.ar/petscfem) primarily targeted to bi-dimensional (2D) and three-dimensional (3D) finite elements computations on general unstructured grids.

Several tests were conducted in order to validate and evaluate the method describing the flow conditions that take place in "real-life" applications, such as inside a low speed wind tunnel test section at high Reynolds number.

1 INTRODUCTION

The generation of random flow field as an inflow boundary condition in large eddy simulations (LES) is a topic that has been widely studied owing to two main reasons. Firstly, LES has become an attractive approach due to the improvement of computational power. Secondly, regarding that the turbulence behavior within the domain is strongly influenced by the inlet conditions; and moreover, considering that even for stationary turbulent flows, if the inlet conditions are not properly prescribed, LES method could demand a high execution time to obtain a fully developed turbulence.

In view of this facts, several methods are available for the generation of inlet turbulence conditions and they follow different approaches that can be classified into two general methodologies: precursor simulation methods and synthesis methods (Tabor and Baba-Ahmedi, 2010). Both approaches presents advantages and drawbacks and can be implemented in many different ways.

Precursor simulation methods involve the generation of turbulence by running a precomputation of the flow in order to generate a 'library' or database, before or in concurrency with the main LES calculation. Then, the generated fluctuations are introduced into the inlet boundary of the computational domain. Examples of this kind of approach are the methods based on *cyclic domains* (Kim et al., 1987; Lund et al., 1998) or those using a *preprepared library*. In particular, Lund et al. (1998) applied their modified Spalart method, in a *concurrent library generation* fashion, sampling the data as the simulation proceed.

All the above mentioned precursor methodologies can be integrated into the main domain, sampling the turbulence in a downstream section of the inlet and then mapping it back into the inlet. In summary, the precursor simulation methods set the conditions for the LES implementation from a 'real' simulation of turbulence, hence it is expected that the velocity fluctuation field could possess many of the required statistical characteristics, including temporal and spatial correlation and energy spectrum.

Another widely used methodology is the so called synthesized turbulence method. In this method a pseudo-random coherent field of fluctuating velocities with spatial and time scales is superimposed on a predefined mean flow. The random perturbations can be generated in several different ways, such as the *Fourier techniques* (with its variants), the *digital filter based method* and the *proper orthogonal decomposition* (POD) analysis (Tabor and Baba-Ahmedi, 2010).

An example of Fourier approaches is the random flow generation (RFG) technique proposed by Smirnov et al. (2001) and developed on the basis of the work of Kraichnan (1970), that involves scaling and orthogonal transformations applied to a continuous flow field. This transient flow field is generated in a three-dimensional domain as a superposition of harmonic functions with random coefficients. The method can generate an isotropic divergence-free fluctuating velocity field satisfying the Gaussian's spectral model as well as an inhomogeneous and anisotropic turbulence flow, provided that an anisotropic velocity correlation tensor is given. Smirnov et al. (2001) used their approach to set inlet boundary conditions to LES methods in the simulation of turbulent fluctuations in a ship wake as well as initial conditions in the simulation of turbulent flow around a ship-hull. Another application successfully tested by the authors was the particle dynamics modeling (Smirnov et al., 2005). It must be noted that the RFG method has been included in the computational fluid dynamics (CFD) software FLUENT and was called *Spectral Synthesizer* (Fluent, 2007).

All the above characteristics were taken into account in the discretizing and synthesizing random flow generation (DSRFG) method by Huang et al. (2010), with the advantage that the

spatially correlated turbulent flow field can satisfy any arbitrary model spectrum. This property is especially useful in computational wind engineering applications where the von Kármán model is widely adopted as a target spectrum and the energy content of the inertial subrange cannot be discarded. Another remarkable feature of this method is its highly parallelizable algorithmic implementation since the generation of the fluctuating velocity series is independent for each node in the inlet plane of the computational domain; to the point that the procedure can be done in an embarrassing parallel way. As this methodology imply discretizing and synthesizing procedures for the generation of the inlet turbulence the authors called this approach as *discretizing and synthesizing random flow generation* (DSRFG) method. The authors concluded that the DSRFG method proved to be able to enhance the accuracy of the turbulent flow simulation and wind-induced forces on the building because of a more realistic vortices production in the inlet turbulence flow. Nevertheless, only a few comments about the statistical characteristics of the synthesized turbulence and no discussion at all about the time correlation was made.

The aim of the present study is to propose a synthesized turbulence method that is essentially a modification of the DSRFG method. We shall focused on the derivation of the mathematical equations used to generate fluctuating velocity series and the statistical implications of its parameters.

2 A MODIFIED METHOD TO SYNTHESIZE INLET TURBULENCE

Huang et al. (2010) proposed a synthesis method called discretizing and synthesizing random flow generation (DSRFG) for the implementation of inlet turbulence conditions to perform LES computations. This method proved to have several advantages with respect to its predecessor, the random flow generation (RFG) by Smirnov (Smirnov et al., 2001). Nevertheless, some re-analysis on the turbulence generative equations performed by the authors of this work demonstrated that some improvements can be made. According to this, a brief introduction of the DSRFG is performed followed by the presentation of the modifications proposed. For a more detailed description about the RFG and DSRFG methods, the reader is encouraged to refer to the original articles.

Following the DSRFG method, a homogeneous and isotropic turbulent flow field $\boldsymbol{u}(\boldsymbol{x},t)$ can be synthesized as follows:

$$u_i(\boldsymbol{x},t) = \sum_{m=1}^{M}\sum_{n=1}^{N}[p_i^{m,n}\cos(\tilde{k}_j^{m,n}\tilde{x}_j + \omega_{m,n}t) + q_i^{m,n}\sin(\tilde{k}_j^{m,n}\tilde{x}_j + \omega_{m,n}t)], \tag{1}$$

where

$$\mathbf{p}^{m,n} = \frac{\boldsymbol{\zeta}\times\mathbf{k}^{m,n}}{|\boldsymbol{\zeta}\times\mathbf{k}^{m,n}|}\sqrt{a\frac{4E(k_m)}{N}}, \tag{2}$$

$$\mathbf{q}^{m,n} = \frac{\boldsymbol{\xi}\times\mathbf{k}^{m,n}}{|\boldsymbol{\xi}\times\mathbf{k}^{m,n}|}\sqrt{(1-a)\frac{4E(k_m)}{N}}, \tag{3}$$

$$\tilde{\mathbf{x}} = \frac{\mathbf{x}}{L_s}, \tag{4}$$

$$\tilde{\mathbf{k}}^{m,n} = \frac{\mathbf{k}^{m,n}}{k_0}, \tag{5}$$

with $\omega_{m,n} \in N(0, 2\pi f_m)$, $f_m = k_m U_{\text{avg}}$, $\boldsymbol{\zeta}$ and $\boldsymbol{\xi}$ are the vector form of ζ_i^n and ξ_i^n, which are random numbers selected independently from $N(0,1)$. L_s in equation (4) is a scale factor

related to the length scale of turbulence and plays an important role in this formulation, as will be further specified later.

The factors $p_i^{m,n}$ and $q_i^{m,n}$ defines the distribution of the three dimensional energy spectrum $E(k_m)$ in each of the spatial coordinate axes which in turn are functions of the space wave number $\mathbf{k}^{m,n}$ ($|\mathbf{k}^{m,n}| = k_m$) and normal random vectors $\boldsymbol{\zeta}$ and $\boldsymbol{\xi}$. When dealing with homogeneous and isotropic turbulence, the distribution of $\mathbf{k}^{m,n}$ is isotropic on the surface of a sphere and consequently the energy is uniformly distributed in the space. In such conditions it is evident that the same spectrum will be obtained in the three principal directions but in the case of inhomogeneous and anisotropic turbulence the distribution of $\mathbf{k}^{m,n}$ must change according to the conditions of inhomogeneity and anisotropy. To achieve this behavior, $p_i^{m,n}$ and $q_i^{m,n}$ must be *aligned* with the energy spectrum along a principal direction and then the distribution of $\mathbf{k}^{m,n}$ can be *remapped* on the surface of the sphere. To summarize, the method is implemented using equation (1) and

$$p_i^{m,n} = \operatorname{sign}(r_i^{m,n}) \sqrt{\frac{4}{N} E_i(k_m) \frac{(r_i^{m,n})^2}{1 + (r_i^{m,n})^2}}, \tag{6}$$

$$q_i^{m,n} = \operatorname{sign}(r_i^{m,n}) \sqrt{\frac{4}{N} E_i(k_m) \frac{1}{1 + (r_i^{m,n})^2}}, \tag{7}$$

$$\mathbf{k}^{m,n} \cdot \mathbf{p}^{m,n} = 0, \tag{8}$$

$$\mathbf{k}^{m,n} \cdot \mathbf{q}^{m,n} = 0, \tag{9}$$

$$|\mathbf{k}^{m,n}| = k_m, \tag{10}$$

where $r_i^{m,n}$ is a random number, independently selected from a three dimensional Normal distribution with $\mu_r = 0$ and $\sigma_r = 1$.

Here, with the aim to expose the ideas behind the proposed modifications we introduce some considerations about the statistical implications of the DSRFG method. The mean square value of equation (1) in each direction $i = 1, 2, 3$ can be written as:

$$u_{\mathrm{rms},i}^2(\boldsymbol{x}, t) = \lim_{T\to\infty} \frac{1}{T} \int_0^T \Big\{ \sum_{m=1}^{M} \sum_{n=1}^{N} [p_i^{m,n} \cos(\tilde{k}_j^{m,n} \tilde{x}_j + \omega_{m,n} t) + q_i^{m,n} \sin(\tilde{k}_j^{m,n} \tilde{x}_j + \omega_{m,n} t)] \Big\}^2 dt. \tag{11}$$

that is,

$$\lim_{T\to\infty} \int_0^T \Big[\sum_{m=1}^{M} \sum_{n=1}^{N} (\alpha_{m,n} + \varphi_{m,n}) \Big]^2 dt = \lim_{T\to\infty} \int_0^T \Big(\sum_{m=1}^{M} \sum_{n=1}^{N} \alpha_{m,n} \Big)^2 dt + \lim_{T\to\infty} \int_0^T \Big(\sum_{m=1}^{M} \sum_{n=1}^{N} \varphi_{m,n} \Big)^2 dt, \tag{12}$$

where

$$\begin{aligned} \alpha_{m,n} &= p_i^{m,n} \cos(\tilde{k}_j^{m,n} \tilde{x}_j + \omega_{m,n} t) \\ \varphi_{m,n} &= q_i^{m,n} \sin(\tilde{k}_j^{m,n} \tilde{x}_j + \omega_{m,n} t), \end{aligned} \tag{13}$$

Furthermore, equation (12) can be expressed as

$$\begin{aligned}\lim_{T\to\infty}\frac{1}{T}\int_0^T\Big[\sum_{m=1}^{M}\sum_{n=1}^{N}(\alpha_{m,n}+\varphi_{m,n})\Big]^2dt \\ =\lim_{T\to\infty}\frac{1}{T}\sum_{m=1}^{M}\sum_{n=1}^{N}\int_0^T\alpha_{m,n}^2dt+\lim_{T\to\infty}\frac{1}{T}\sum_{m=1}^{M}\sum_{n=1}^{N}\int_0^T\varphi_{m,n}^2dt,\end{aligned} \tag{14}$$

Then, using the result of equation (14) and by virtue of equations (11) and (13):

$$\begin{aligned}u_{\mathrm{rms},i}^2(\boldsymbol{x},t)&=\lim_{T\to\infty}\frac{1}{T}\int_0^T\Big[\sum_{m=1}^{M}\sum_{n=1}^{N}(\alpha_{m,n}+\varphi_{m,n})\Big]^2dt \\ &=\frac{1}{2}\sum_{m=1}^{M}\sum_{n=1}^{N}[p_i^{m,n}]^2+\frac{1}{2}\sum_{m=1}^{M}\sum_{n=1}^{N}[q_i^{m,n}]^2.\end{aligned} \tag{15}$$

Summing the left and right hands for $i=1,2,3$,

$$\sum_{i=1}^{3}u_{\mathrm{rms},i}^2(\boldsymbol{x},t)=\frac{1}{2}\sum_{m=1}^{M}\sum_{n=1}^{N}\sum_{i=1}^{3}[p_i^{m,n}]^2+\frac{1}{2}\sum_{m=1}^{M}\sum_{n=1}^{N}\sum_{i=1}^{3}[q_i^{m,n}]^2, \tag{16}$$

or in a more compact form (using Einstein summation convention):

$$\begin{aligned}\overline{u_iu_i}&=\frac{1}{2}\sum_{m=1}^{M}\sum_{n=1}^{N}p_i^{m,n}p_i^{m,n}+\frac{1}{2}\sum_{m=1}^{M}\sum_{n=1}^{N}q_i^{m,n}q_i^{m,n} \\ &=2\int_0^\infty E(k)dk\;\approx\;2\sum_{m=1}^{M}E(k_m)\Delta k_m,\end{aligned} \tag{17}$$

given that the integral of the energy spectrum function $E(k)$ is equal to the energy per unit mass of fluid. According to the definition of $p_i^{m,n}$ and $q_i^{m,n}$ (equations (6) and (7)) it can be seen that

$$\begin{aligned}\overline{u_iu_i}&=\frac{1}{2}\sum_{m=1}^{M}\sum_{n=1}^{N}\sum_{i=1}^{3}\Big[\frac{4}{N}E_i(k_m)\frac{(r_i^{m,n})^2}{1+(r_i^{m,n})^2}+\frac{4}{N}E_i(k_m)\frac{1}{1+(r_i^{m,n})^2}\Big] \\ &=\frac{2}{N}\sum_{m=1}^{M}\sum_{n=1}^{N}E(k_m)=2\sum_{m=1}^{M}E(k_m),\end{aligned} \tag{18}$$

thus, as $E(k_m)$ is a positive quantity for any k, the kinetic energy is represented by a divergent series. This causes a strong dependency of the turbulence intensity of the generated fluctuating velocities with the number of points M considered to discretize the model spectrum.

2.1 Time and spatial correlation

The autocorrelation function can be computed as

$$\begin{aligned}\overline{u_i(\boldsymbol{x},t)u_i(\boldsymbol{x},t+\tau)} &= \lim_{T\to\infty}\frac{1}{T}\int_0^T u_i(\boldsymbol{x},t)u_i(\boldsymbol{x},t+\tau)dt \\ &= \lim_{T\to\infty}\frac{1}{T}\int_0^T \sum_{m=1}^{M}\sum_{n=1}^{N}\Big[p_i^{m,n}\cos(\tilde{k}_j^{m,n}\tilde{x}_j+\omega_{m,n}t)+ \\ &+ q_i^{m,n}\sin(\tilde{k}_j^{m,n}\tilde{x}_j+\omega_{m,n}t)\Big]\sum_{m=1}^{M}\sum_{n=1}^{N}\Big[p_i^{m,n}\cos(\tilde{k}_j^{m,n}\tilde{x}_j+ \\ &+ \omega_{m,n}(t+\tau))+q_i^{m,n}\sin(\tilde{k}_j^{m,n}\tilde{x}_j+\omega_{m,n}(t+\tau))\Big]dt,\end{aligned} \tag{19}$$

then, after some mathematical manipulation using equations (6) and (7),

$$\overline{u_i(\boldsymbol{x},t)u_i(\boldsymbol{x},t+\tau)} = \sum_{m=1}^{M}\sum_{n=1}^{N}\frac{2}{N}E_i(k_m)\cos(\tau\omega_{m,n}). \tag{20}$$

Note that, if $\tau = 0$ then the equation (20) gives back the equation (15).

Likewise, an expression for the spatial correlation can be obtained in an analogous way:

$$\overline{u_i(\boldsymbol{x},t)u_i(\boldsymbol{x'},t)} = \sum_{m=1}^{M}\sum_{n=1}^{N}\frac{2}{N}E_i(k_m)\cos\left[\tilde{k}_j^{m,n}\frac{(x_j'-x_j)}{L_s}\right] \tag{21}$$

Comparing equations (20) and (21), it can be seen that while in the last equation a *scaling parameter* L_s (that provides a way to obtain the required spatial correlation in the generated flow field) exists, an analogous parameter is not present in the first equation.

3 PROPOSED METHODOLOGY

In the light of the analysis above, we propose some modifications to the equations of the DSRFG method. Firstly, the Fourier series in equation (1) will be written as:

$$\begin{aligned}u_i(\boldsymbol{x},t) = \sum_{m=1}^{M}\sum_{n=1}^{N}\Big[&p_i^{m,n}\cos\left(\tilde{k}_j^{m,n}\tilde{x}_j+\omega_{m,n}\frac{t}{\tau_0}\right) \\ &+ q_i^{m,n}\sin\left(\tilde{k}_j^{m,n}\tilde{x}_j+\omega_{m,n}\frac{t}{\tau_0}\right)\Big],\end{aligned} \tag{22}$$

where τ_0 is a parameter introduced to allow some "control" over the time correlation.

Secondly, the parameters $p_i^{m,n}$ and $q_i^{m,n}$ have to be in accordance with equation (17). To decoupling this equation we propose the following relationship:

$$\sum_{i=1}^{3}u_{\mathrm{rms},i}^2 = 2\sum_{m=1}^{M}E(k_m)\Delta k_m = 2\sum_{m=1}^{M}\sum_{i=1}^{3}c_iE_i(k_m)\Delta k_m, \tag{23}$$

where $E_i(k_m)$ is the energy spectrum along direction i and c_i is a function value that depends on the form of the spectrum in order to satisfy the condition

$$u_{\mathrm{rms},i}^2 = 2c_i\int_0^\infty E_i(k)dk, \tag{24}$$

i.e., in each direction the variance of the simulated velocity series must satisfy the equation (24). Then,

$$\sum_{i=1}^{3} u_{\mathrm{rms},i}^2 = 2\sum_{i=1}^{3}\int_0^\infty c_i E_i(k)\Delta k = 2\int_0^\infty E(k)\Delta k. \tag{25}$$

Thus, for each direction i we obtain the modified values of equations (6) and (7):

$$p_i^{m,n} = \mathrm{sign}(r_i^{m,n})\sqrt{\frac{4c_i}{N}E_i(k_m)\Delta k_m \frac{(r_i^{m,n})^2}{1+(r_i^{m,n})^2}}, \tag{26}$$

$$q_i^{m,n} = \mathrm{sign}(r_i^{m,n})\sqrt{\frac{4c_i}{N}E_i(k_m)\Delta k_m \frac{1}{1+(r_i^{m,n})^2}}. \tag{27}$$

Now, equation (20) can be written as

$$\overline{u_i(\boldsymbol{x},t)u_i(\boldsymbol{x},t+\tau)} = \frac{2c_i}{N}\sum_{m=1}^{M}\sum_{n=1}^{N} E_i(k_m)\Delta k_m \cos\left(\frac{\tau}{\tau_0}\omega_{m,n}\right), \tag{28}$$

while equation (21) changes to

$$\overline{u_i(\boldsymbol{x},t)u_i(\boldsymbol{x'},t)} = \frac{2c_i}{N}\sum_{m=1}^{M}\sum_{n=1}^{N} E_i(k_m)\Delta k_m \cos\left[\tilde{k}_j^{m,n}\frac{(x_j'-x_j)}{L_s}\right]. \tag{29}$$

The spatial scaling parameter L_s is obtained by

$$L_s = \theta_1\sqrt{L_u^2+L_v^2+L_w^2}, \tag{30}$$

and the time scaling parameter τ_0 can be derived using the Taylor's hypothesis, so that

$$\tau_0 = \theta_2\frac{L_s}{U_{\mathrm{avg}}}. \tag{31}$$

θ_1 and θ_2 are scalars to be defined according to the problem at hands. Since this new methodology is based on the DSRFG approach, we called it as *modified discretizing and synthesizing random flow generation* (MDSRFG).

4 VALIDATION OF THE PROCEDURE

A test case, considering inhomogeneous anisotropic turbulent conditions of the flow field, was performed. This example was proposed Huang et al. (2010). The spectra of the three principal velocity components are described by the von Kármán models, i.e.,

$$S_u(f) = \frac{4(I_u U_{\mathrm{avg}})^2(L_u/U_{\mathrm{avg}})}{[1+70.8(fL_u/U_{\mathrm{avg}})^2]^{5/6}}, \tag{32}$$

$$S_v(f) = \frac{4(I_v U_{\mathrm{avg}})^2(L_v/U_{\mathrm{avg}})(1+188.4(2fL_v/U_{\mathrm{avg}})^2)}{[1+70.8(2fL_v/U_{\mathrm{avg}})^2]^{11/6}}, \tag{33}$$

$$S_w(f) = \frac{4(I_w U_{\mathrm{avg}})^2(L_w/U_{\mathrm{avg}})(1+188.4(2fL_w/U_{\mathrm{avg}})^2)}{[1+70.8(2fL_w/U_{\mathrm{avg}})^2]^{11/6}}. \tag{34}$$

The turbulence intensity values are $I_u = 8\%$, $I_v = 16\%$ and $I_w = 24\%$, while the turbulence integral length scales are $L_u = 0.6$ m, $L_v = 0.3$ m and $L_w = 0.1$ m. To apply the procedure we must first obtain the c_i values of equations (26) and (27) using the relationship (24), that is

$$\begin{aligned} u^2_{\text{rms},1} = (I_u U_{\text{avg}})^2 &= 2c_1 \int_0^\infty S_u(k)dk \\ &\approx 2c_1\, 0.2377\, \beta\Big(\frac{1}{3},\frac{1}{2}\Big) I_u^2 U_{\text{avg}} \quad \Rightarrow \quad c_1 = \frac{U_{\text{avg}}}{2}, \end{aligned} \tag{35}$$

where $\beta(,)$ is the Beta function (Abramowitz and I., 1970). In the same way, c_2 and c_3 are such that,

$$\begin{aligned} u^2_{\text{rms},2} = (I_v U_{\text{avg}})^2 &= 2c_2 \int_0^\infty S_v(k)dk \\ &\approx 2c_2 \left[0.1189\, \beta\Big(\frac{1}{2},\frac{4}{3}\Big) + 0.3163\, \beta\Big(\frac{1}{3},\frac{3}{2}\Big)\right] I_v^2 U_{\text{avg}} \\ &\Rightarrow \quad c_2 = c_3 \approx \frac{U_{\text{avg}}}{2}. \end{aligned} \tag{36}$$

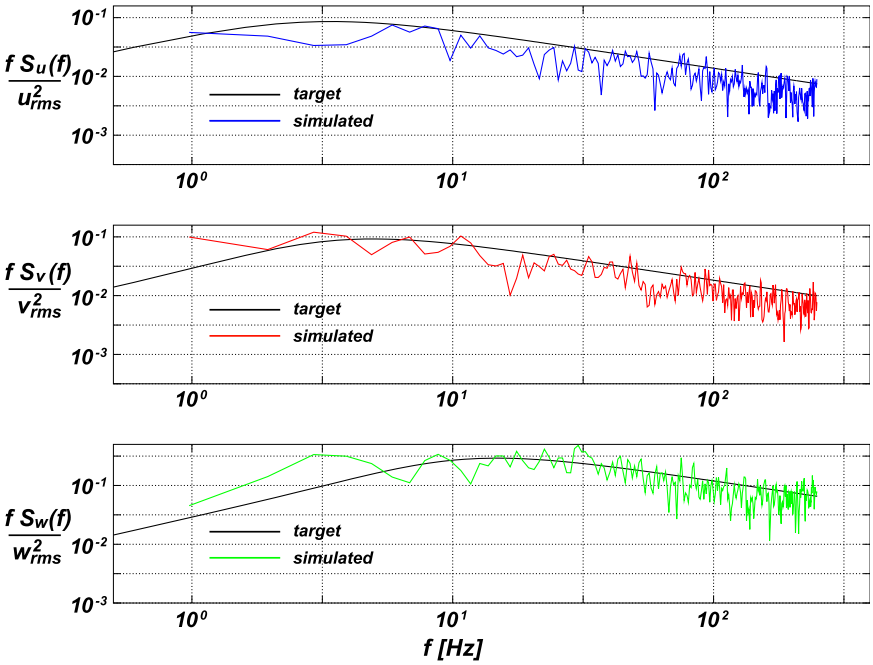

Figure 1: Comparison of the spectra simulated by the modified DSRFG with the target spectra.

As can be observed in figure (1) the simulated spectra fit well with the target spectra in the three principal directions; indicating that the anisotropy of the spectra is well represented by the proposed method. The rms value of each simulated fluctuating velocity component (obtained from a sample of 10 velocity simulations) is also compared to corresponding target values. As shown in table (1) the fluctuating velocities simulated by the MDSRFG approach is in better agreement with the target values obtained using the *scaling and orthogonal transformation* or the *aligning and remapping* techniques (Huang et al., 2010).

	σ_u	σ_v	σ_w
Scaling and transformation	0.9968	2.44	2.9956
Aligning and remapping	0.95	1.9987	3.08
MDSRFG approach	1.0527	2.1850	3.1123
target	1.12	2.24	3.36

Table 1: Comparison of the rms values [m/s] of the simulated fluctuating velocities by different techniques.

When modeling the spatial correlation between same fluctuating velocity components in two different points i and j, a spatial correlation matrix needs to be computed. This target function is built for the u-component, for instance, from the spectra and coherence functions between nodes i and j as

$$\boldsymbol{S}_{\boldsymbol{c}i,j} = \sum_{m=1}^{M} \sqrt{Su^i(f_m) Su^j(f_m)}\, \gamma_u^y(f_m), \tag{37}$$

where

$$\gamma_u^y(f_m) = \exp\Big(\frac{-C_u^y |y_i - y_j| f_m}{U_{\text{avg}}}\Big), \tag{38}$$

is the coherence function of the u fluctuating velocity component in the $y-$direction and C_u^y is the decay coefficient (usually taken in the range 10-12).

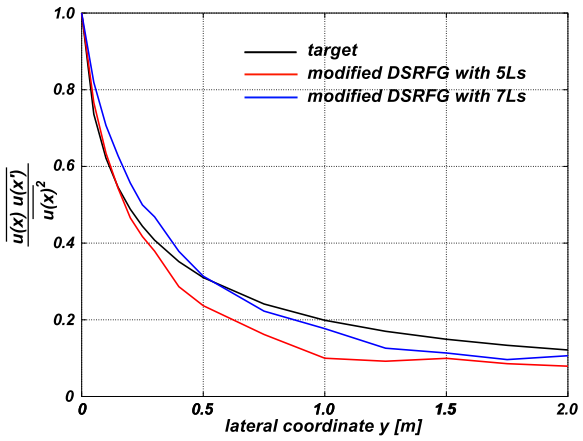

Figure 2: Non-dimensional spatial correlation of the u fluctuating velocity component.

In figures (2), (3) and (4) the spatial correlation for the u, v and w-components of the velocity fluctuations obtained by the expression (29) is compared to correlations computed using equation (37) for different values of L_s.

Time correlation is also computed for each velocity component according to equation (28) and compared to the expression

$$R(m\delta\tau) = \frac{1}{M-m} \sum_{j=0}^{M-m} u_i(j\ \delta\tau)\ u_i[(j+m)\ \delta\tau], \tag{39}$$

here, m is an integer such that $\tau_m = m\delta\tau$, with $0 \leq m < M$ and M is the length of the vector τ_m. Comparing the results shown in figures (5), (6) and (7) it can be seen that the temporal correlations of the each component are well represented by the simulated series.

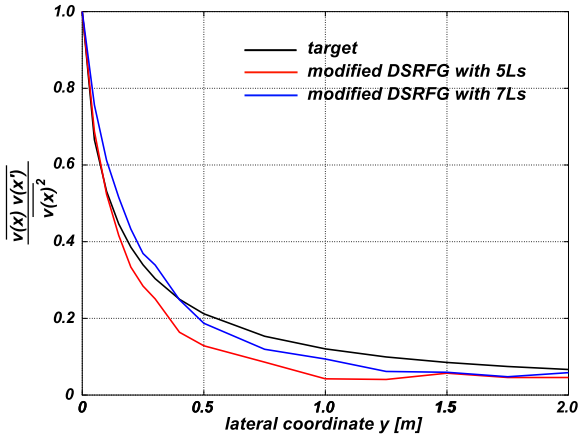

Figure 3: Non-dimensional spatial correlation of the v fluctuating velocity component.

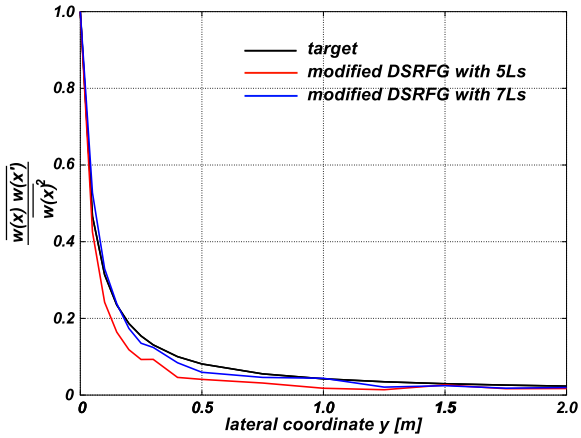

Figure 4: Non-dimensional spatial correlation of the w fluctuating velocity component.

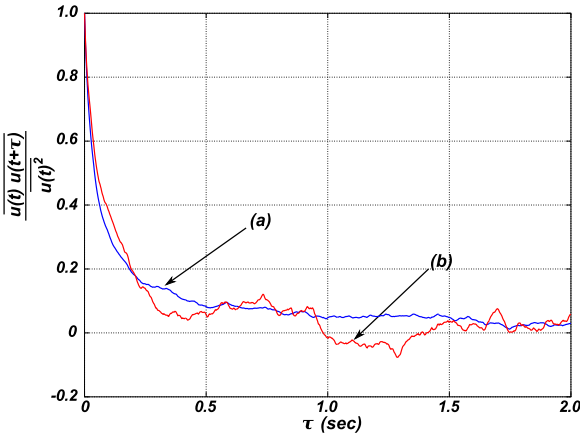

Figure 5: Non-dimensional time correlation of the u fluctuating velocity component. *(a)* equation (28), *(b)* equation (39).

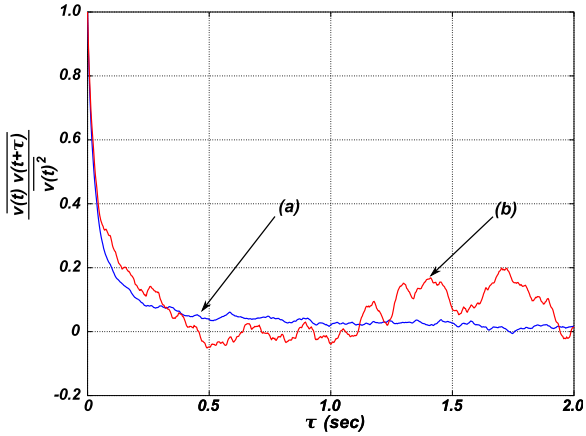

Figure 6: Non-dimensional time correlation of the v fluctuating velocity component. *(a)* equation (28), *(b)* equation (39).

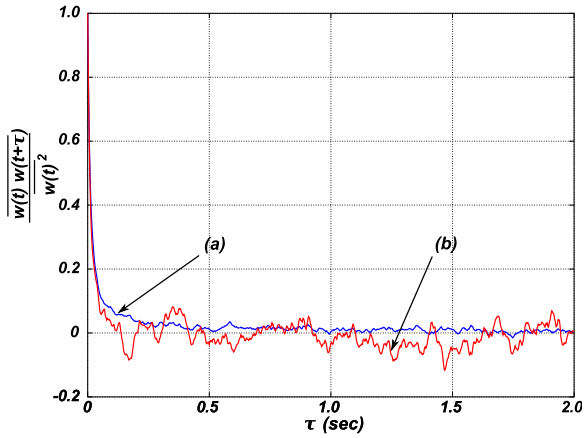

Figure 7: Non-dimensional time correlation of the w fluctuating velocity component. *(a)* equation (28), *(b)* equation (39).

Some remarks

As it is clearly depicted by equation (22) the computational cost is identical as in the DSRFG method. Thus, for each node at the inlet section the cost at each time step is $O(MN)$; where M is the number of points in which the target spectrum is discretized and N the number of samples for each wave number k_m. A remarkable feature of the algorithm is evidenced by noting that the computation of the fluctuating velocity components in equation (22) is independent of LES process, i.e., the turbulence synthesis for some number of time steps (or the entire simulation process) can be done prior to the LES computations.

The anisotropic turbulence conditions at the inlet plane can be obtained by performing a previous RANS simulation or by experimental measurements. The two input parameters, L_s and τ_0, must be carefully selected (at least in a few inlet nodes) in order reproduce the statistical properties of the flow under consideration.

As a final observation we notice that the proposed approach, as any synthesized turbulence generation method, must be used as a turbulence initializer, i.e., a perturbation generator that "triggers" the transition to a fully developed turbulence state by LES (Davidson, 2007). In this regard, it must be said that independently of the selected L_s value, the resolved scales are in concordance with the mesh (filter) size which is inherent to the LES conception.

5 APPLICATION OF THE MODIFIED DSRFG METHOD IN LES

It is well known that the generation of developed turbulence by LES at high Reynolds number flows is computationally expensive and time consuming. A particular field where those two flow conditions meet is in the study of computational aerodynamics of buildings, bridges, airplanes and all kind of road vehicles. In order to avoid the drawbacks mentioned above, the MDSRFG method can be used to setting up the turbulent inflow conditions in LES computations.

As an example of application, a computational simulation of the flow conditions in the *UNNE Wind Tunnel* test section was performed. This wind tunnel is an open-circuit, low velocity atmospheric boundary layer wind tunnel. The flow characteristics of the test section, defining the input data for the MDSRFG method, were taken from the work of Wittwer and Möller (2000).

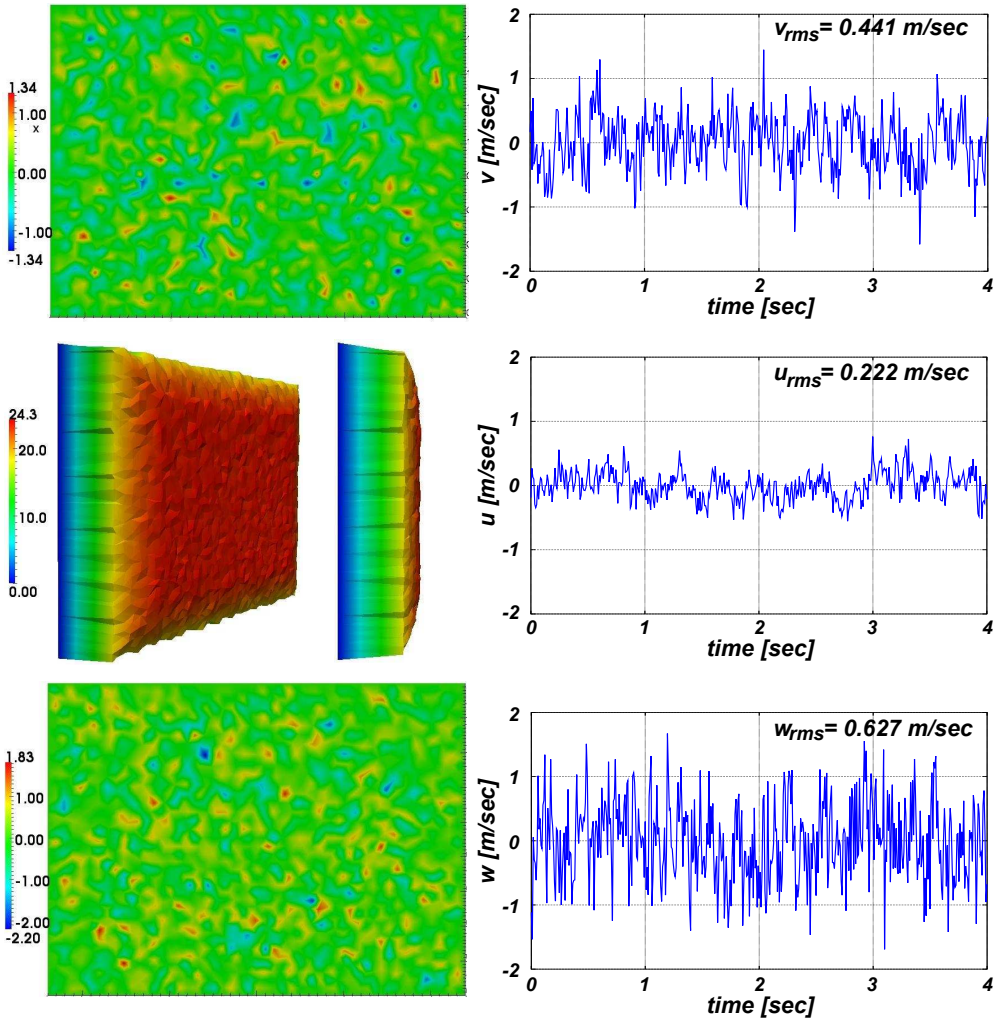

Figure 8: Inlet fluctuating velocities simulated by the MDSFRG method.

Other parameters, like turbulence intensities $I_v = 0.02$, $I_w = 0.03$, integral length scales $L_u = 0.3$ m, $L_v = 0.1$ m, $L_w = 0.05$ m and the mean velocity magnitude of 23.6 m/s were also adopted. The input parameters for the MDSRFG method presented in equations (30) and (31) were computed with $\theta_1 = 45$ and $\theta_2 = 0.5\pi$. The domain was a rectangular box with a cross section of 2.40 m width (x-direction) and a height of 1.80 m (z-direction) representing the wind

tunnel test section. Non-slip boundary condition is prescribed at ground, roof and tunnel walls, while null pressure is imposed at outlet wall.

The computational simulations were performed using the PETSc-FEM code developed at the CIMEC (http://www.cimec.org.ar/petscfem). PETSc-FEM is a general purpose, parallel, multi-physics finite element program which has been used in many applications including analysis of petroleum refinery processes, aerospace industry, environmental impact assessment and siderurgical processes. PETSc-FEM uses the Finite Element Method (FEM) to solve the momentum and continuity equations for the velocity and pressure at each node and at each time step on unstructured meshes. Streamline-Upwind/Petrov-Galerkin (SUPG) (Brooks and Hughes, 1982) and the Pressure-Stabilizing/Petrov-Galerkin (PSPG) (Tezduyar, 1992) discretization scheme of the incompressible Navier-Stokes equations were implemented. The problem was solved using a Beowulf kind of cluster architecture with disk-less dual quad-core Intel Xeon E5420 (1333Mhz Front Side Bus, FSB) processors (2.5 GHz CPU with 8 Gb RAM per node) interconnected via a Gigabit Ethernet network.

Figure (8) shows in the right side the time history of the simulated fluctuating velocity components in a central point of the inlet section and the instantaneous fluctuation contours on the left side. The velocities maintains the spatial anisotropy among the three directions, as can be observed from the statistical values.

6 CONCLUSIONS

In this paper, a general method for the generation of inflow synthesized turbulence was presented and evaluated. The method is based on a previously turbulence generator known as the discretizing and synthesizing random flow generation (DSRFG) method, preserving its main characteristics and advantages. The key point of the modified DSRFG (MDSRFG) method presented in this study is that it preserves the statistical quantities that would be prescribed at the inlet of the domain independently of the number of samples M (number of points in the spectrum) considering in the computation of the factors $p_i^{m,n}$ and $q_i^{m,n}$ of equation (22) by virtue of the proposed equations (26) and (27).

As each fluctuating velocity component is generated in each node independently of the others, the method is highly parallelizable. Furthermore, the generation of each nodal fluctuating velocity component can be done previously to the computation by LES, calling in each time step the corresponding nodal value.

It is worthy noting that the grid resolution in this transition region needs to be an adequate one in order to ensure that the high frequency turbulence statistics imposed in the inlet conditions will not be filtered by the size of the cells.

7 ACKNOWLEDGMENTS

This work has received financial support from *Consejo Nacional de Investigaciones Científicas y Técnicas* (CONICET, Argentina, grant PIP 5271/05, PIP 112-200801-2956), *Universidad Nacional del Litoral* (UNL, Argentina, grant CAI+D 2009 65/334), *Agencia Nacional de Promoción Científica y Tecnológica* (ANPCyT, Argentina, grants PICT 01141/2007, PICT 0270/2008, PICT-1506/2006) and was partially performed with the Free Software Foundation GNU-Project resources as GNU/Linux OS, GCC compilers, GNU/Octave, as well as the other Open Source resources as Python, Perl, VTK, PETSc, MPICH, Open-DX, Paraview, LATEX and JabRef, among many others.

REFERENCES

Abramowitz M. and I. S. *Handbook of Mathematical Functions: with Formulas, Graphs, and Mathematical Tables*. Dover Publications, 1970.

Brooks A. and Hughes T. Streamline upwind/petrov-galerkin formulations for convection dominated flows with particular emphasis on the incompressible navier-stokes equations. *Computer Methods in Applied Mechanics and Engineering*, 32:199–259, 1982.

Davidson L. Using isotropic synthetic fluctuations as inlet boundary conditions for unsteady simulations. *Advances and Applications in Fluid Mechanics*, 1(1):1–35, 2007.

Fluent. *Fluent 6.3 User's Guide*, 2007.

Huang S.H., Li Q.S., and Wu J.R. A general inflow turbulence generator for large eddy simulation. *Journal of Wind Engineering and Industrial Aerodynamics*, 98:600–617, 2010.

Kim J., Moin P., and Moser R. Turbulence statistics in fully developed channel flow at low reynolds number. *Journal of Fluid Mechanics*, 177:133–166, 1987.

Kraichnan R.H. Diffusion by a random velocity field. *The Physics of Fluids*, 13:22–31, 1970.

Lund T.S., Wu X., and Squires K.D. Generation of turbulent inflow data for spatially-developing boundary layer simulations. *Journal of Computational Physics*, 140:233–258, 1998.

Smirnov A., Celik I., and Shi S. Les of bubble dynamics in wake flows. *Computers and Fluids*, 34:351–373, 2005.

Smirnov A., Shi S., and Celik I. Random flow generation technique for large eddy simulations and particle-dynamics modeling. *Journal of Fluids Engineering*, 123:359–371, 2001.

Tabor G. and Baba-Ahmedi M. Inlet conditions for large eddy simulation: A review. *Computers and Fluids*, 39:553–567, 2010.

Tezduyar T. Stabilized finite element formulations for incompressible flow computations. *Advances in Applied Mechanics*, 28:1–44, 1992.

Wittwer A. and Möller S. Characteristics of the low speed wind tunnel of the unne. *Journal of Wind Engineering and Industrial Aerodynamics*, 84:307–320, 2000.